

A robust spike and wave algorithm for detecting seizures in a genetic absence seizure model

Petros Xanthopoulos, Chang-Chia Liu, Jicong Zhang, Eric R. Miller, S. P. Nair, Basim M. Uthman, Kevin Kelly, and Panos M. Pardalos

Abstract—Animal Models are used extensively in basic epilepsy research. In many studies, there is a need to accurately score and quantify all epileptic spike and wave discharges (SWDs) as captured by electroencephalographic (EEG) recordings. Manual scoring of long term EEG recordings is a time-consuming and tedious task that requires inordinate amount of time of laboratory personnel and an experienced electroencephalographer. In this paper, we adapt a SWD detection algorithm, originally proposed by the authors for absence (petit mal) seizure detection in humans, to detect SWDs appearing in EEG recordings of Fischer 334 rats. The algorithm is robust with respect to the threshold parameters. Results are compared to manual scoring and the effect of different threshold parameters is discussed.

I. INTRODUCTION

ANIMAL modeling of absence (petit mal) seizures has been conducted in numerous studies using mice and rats. The defining EEG event in these models is a 7-12 Hz generalized spike and wave discharge (SWD; Fig. 1A). In general, SWDs are episodes of abrupt onset, variable duration (seconds to minutes), and abrupt termination that usually occur during passive wakefulness and light sleep [3] [18]. The episodes are characterized by behavioral arrest and decreased responsiveness, with or without rhythmic whisker twitching [2] [18]. Additional behavioral features that may accompany SWDs include accelerated breathing, head tilt, eye twitching [3], and head and neck twitching associated with gradual head lowering [8].

Studies of generalized SWDs are divided into two categories. Acquired SWD models are based upon the use of chemical agents to stimulate the expression of SWDs, or to decrease the threshold for their expression. Spontaneous SWD models, by contrast, are based upon inherited factors that lead to the development of unprovoked generalized

SWD activity. Included in this category are WAG/Rij rats (Wistar Albino Glaxo strain, bred in Rijswijk, Netherlands) and genetic absence epilepsy rats from Strasbourg (GAERS), two Wistar-derived rat strains that have been selectively inbred to increase their propensity to express generalized SWDs [5]. A majority of generalized SWD studies have been performed using these rat strains; however, SWDs can be seen in many common laboratory rat strains, both inbred and outbred. Wistar-unrelated inbred strains include Fischer 344 (F344), Brown Norway, and dark agouti [3] [14] [18]. Common outbred strains include Sprague-Dawley, Wistar, and Long-Evans [2] [12] [16] [18].

Recently data mining, signal processing, and optimization have been used to provide increasing numbers of decision-assisting tools to clinical and basic researchers [10] [11]. Animal models of absence seizures frequently require accurate scoring and quantification of the absence events (SWDs) [6] [7] [8] [9]. This task is usually performed manually by laboratory personnel and an experienced electroencephalographer; manual scoring is a time-consuming and tedious task and is always subject to detection errors due to examiner experience and fatigue. Therefore, an improved automated SWD algorithm is very desirable.

There are very few studies in the literature related to automated SWD detection in animal models. In [17] an automatic SWD detector was introduced based on the first derivative of EEG signals, called the “steepness of the signals.” The SWDs are detected when the value of steepness exceeds the threshold value in certain consecutive EEG epochs. Despite the reported high accuracy of this method, it sometimes misclassifies eye movement artifacts as absence seizures. In [4] Fanselow et al. described a method based on the maximum absolute value of the EEG amplitude in the rat model; the SWDs in the EEG recordings were labeled when the amplitude was greater than the threshold for a manually-defined time horizon [4]. Again, this method could not distinguish between SWDs and high amplitude artifacts. A so-called “spectral comb-based” analytical method was proposed by [15] and used for detecting SWDs in EEG recordings using the GAERS strain. The authors used the time frequency spectrum produced by Short Time Fourier Transform (STFT) to extract features that enabled seizure detection.

In this paper, we adapt the algorithm previously proposed by the authors for automatic detection and quantification of SWD epochs in human absence epilepsy [19] to a rat model

Manuscript received April 23, 2009. This work was partially supported by the NSF, the U.S. Air Force, the North Florida/South Georgia Veterans Health System, an Epilepsy Foundation Research Initiative for Seniors Award (SPN), and NINDS R01 NS046015 (KMK).

P. Xanthopoulos, J-C, Zhang and P. M. Pardalos are with Industrial and Systems Engineering Department at University of Florida, 303 Weil Hall, Gainesville, FL 32611, USA (phone: 352-870-9176; fax: 352-392-3537; e-mail: petros.xanthopoulos@gmail.com).

C-C, Liu, was with Department of Neurosurgery, Medical School of Johns Hopkins University, Baltimore, MD 21287, USA.

Eric R. Miller, S. Nair and K. Kelly are with Allegheny-Singer Research Institute, Allegheny General Hospital, Pittsburgh, PA 15212, USA.

B. M. Uthman was with Weill Cornell Medical College in Qatar, Doha, Qatar.

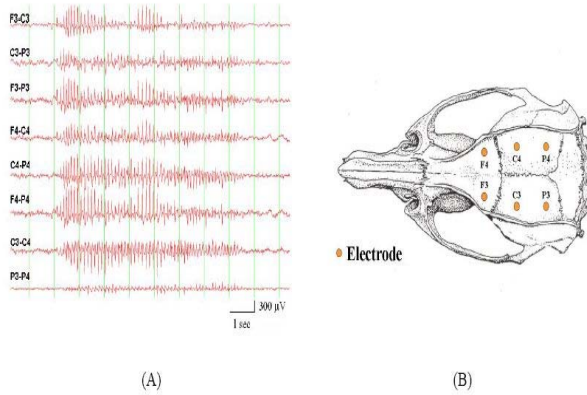


Fig. 1. (A) Sample of a generalized SWD recorded from a Fischer 344 rat. The F3, C3, and P3 abbreviations refer to skull screw electrodes overlying left frontal, central, and parietal regions of the animal’s brain, respectively; F4, C4 and P4 refer to the brain areas on the right. An “F3-C3” label corresponds to an EEG channel produced by the output of one differential amplifier with inputs from the F3 and C3 electrodes. (B) Electrode placement used in the study.

of absence epilepsy. The paper is organized as follows: 1) in section II, we describe the methodology followed by a description of the dataset and the algorithm; 2) in section III, we present the results together with the analysis related to the robustness of the algorithm; and 3) in section IV, we discuss the results and the choice of the threshold parameters.

II. METHODS

A. Dataset description

Eight-hour recordings were acquired from total four 4-month old F344 rats. In total, 6 screw electrodes were implanted in the skull of each animal: 2 frontal (F3, F4), 2 central (C3, C4), and 2 parietal (P3, P4). The electrode configuration is shown in Fig. 1B. In total, 8 differential channels were computed for the purpose of the study: F3-C3, C3-P3, F3-P3, F4-C4, C4-P4, F4-P4, C3-C4, P3-P4 (Fig. 1A). Entire long term video-EEG recordings were visually scanned by laboratory research assistants to detect and score SWD occurrence; identified SWDs were confirmed by an electroencephalographer. The exact number of epochs and their cumulative time during the 8 hours of recordings can be seen in the Table I.

TABLE I
NUMBER OF SWD EPOCHS SCORED FOR EACH RAT AND THE CUMMULATIVE TIME OF SWDS DURING THE 8-HOUR RECORDINGS

	Number of SWD epochs	Cummulative ictal activity (epochs)	Total recording time(hours)
Rat A	53	99.33	8.27
Rat B	43	116.35	8.09
Rat C	81	368.53	8.00
Rat D	45	133.50	8.10
Total	202	717.71	32.46

B. Algorithm

For detecting SWD discharges in a rat model, we propose a modification of our algorithm originally proposed for automatic SWD detection in human data [19]. The proposed detection scheme is based in time frequency decomposition of the EEG employing the wavelet transform. Wavelet transform has profound advantages over the classical STFT because one can increase the scale (or frequency) resolution while keeping the same time resolution. Subsequently, the variance profile of the EEG is computed and seizures are detected by a double thresholding process. The algorithm was found to have high sensitivity and a minimal false positive detection rate for SWDs localized in the frequency band of ~3Hz. Here we describe our detection algorithm in three simple steps.

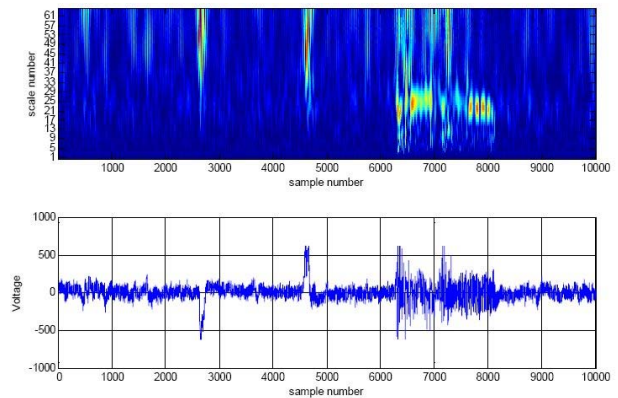


Fig. 2. Typical absence seizure and the corresponding scalogram prior to the seizure (onset after sample 6000). Two electrode artifacts (onset after samples 2000 and 4000) were rejected by keeping only the scales (a=19-25) that correspond to the frequency band of interest

1) *Wavelet decomposition*: First, we decompose every differential channel of the raw EEG recordings, which can be represented as a time series $X(t)$, into a time-scale domain using the wavelet transform: $C(t, a, b) = \int_{-\infty}^{\infty} x(t) \psi_{a,b}(t) dt$, where $\psi_{a,b}(t) = \frac{1}{\sqrt{a}} \psi\left(\frac{t-b}{a}\right)$. The function $\psi(\cdot)$ is the mother wavelet function. For this study, we used the Morlet mother wavelet function, which has analytic expression given by: $\psi(t) = \cos(3\pi t)$. Morlet mother wavelet is used extensively in EEG analysis due to its minimum time-bandwidth product, its infinite differentiation, and its explicit expression [1]. A time scale plot of a recorded absence seizure is shown in Fig. 2.

We can convert scales into frequencies using $f_c = \frac{f_0}{a}$, where f_0 is the central frequency of the mother wavelet, in our case, 0.81Hz, and $\Delta t = \frac{1}{200}$ sec is the sampling period. Among all the scales that we can decompose the EEG signal, we are interested in those that correspond to the frequency band in which SWD activity appears (~7 Hz). For this we keep only the scales 19-25 and sum them for every channel (Fig. 3).

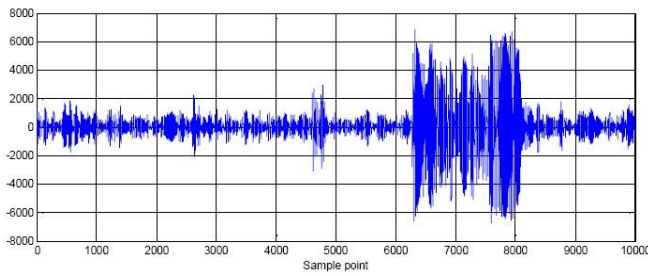


Fig. 3. Sum of scales of interest (19 to 25)

2) *Variance profile computation*: Based on the observation that the high SWD activity produces wavelet profiles of high variance, we compute the variance profile for each channel using a sliding window of width $k=200$ samples (i.e., corresponding to 1 sec of recording). All variance profiles for all channels are summed to reject noise and artifacts that are not generalized (i.e., not appearing in all channels). A variance profile of the seizure can be seen in Fig. 4 (blue line).

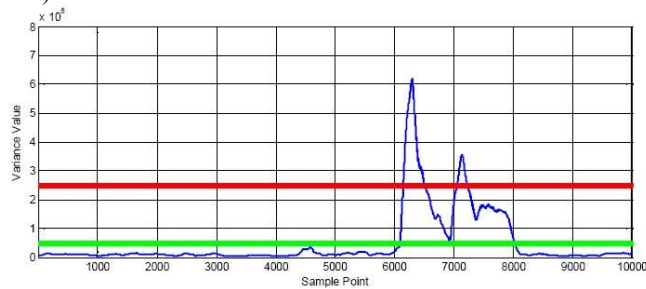


Fig. 4. High threshold illustrated in red detects two distinct epochs of SWDs. For each epoch detected, we try to find the nearest point at which the variance value drops below the low threshold. First thresholding detects two distinct epochs that are merged by the low thresholding search.

3) *Thresholding*: For accurate localization of the onset and offset times of a seizure based on the variance profile of the EEG recordings, we used a double thresholding technique (Fig. 4). We applied a high threshold to the variance to detect the number of epochs; the high threshold was chosen, in part, to avoid detection of artifacts (false positives).

For the sample points of the variance profile curve that “hit” the high threshold, we perform a local search to specify the exact onset and offset sample points of the seizure. More precisely, with reference to Fig 4, for the first point that corresponds to an offset (first point that high line hits the variance profile), we search backwards to determine the first time that the variance curve falls below the low threshold (first point that low threshold intersects with variance profile). For the second point, we search forward to determine the first point that the variance curve drops below the low threshold. For the third and fourth points, we repeat the same search process (third point will correspond again to an onset and the fourth point to an offset). It is worth noting that with the low thresholding search we are able to merge epochs that were detected as two distinct events from the high thresholding (i.e., in this example the onset and the

offset of both epochs will be the same). Finally, the algorithm returns only the unique events (it rejects duplicates).

III. RESULTS

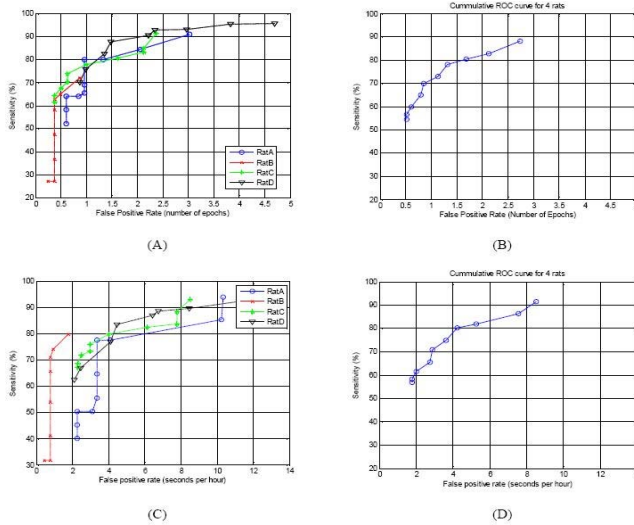
The detection sensitivity and false positive rate are highly dependent on the parameters of the algorithm (thresholds). We experimented with different thresholds to: 1) investigate the robustness of the algorithm, i.e., the change of the output with small changes of the input parameters; and 2) describe how the sensitivity versus specificity changes with respect to the input parameters. For these aims the algorithm was applied using 10 different thresholds and sensitivity and specificity were computed. Sensitivity was defined as the number of epochs detected over the total number of scored epochs, and false positive rate was defined as the number of false positives over the corresponding recording time.

The plot of sensitivity versus specificity is the so-called receiver operating characteristic (ROC) curve. The ROC is very useful in visualizing how the sensitivity percentage changes as a function of missed seizure rate and help the end user to decide the optimal point (corresponding threshold) that fits a specific application. In Fig. 5 (A&B), one can see the ROC curves for the four rats separately and the mean curve for all four rats.

One drawback of this definition of sensitivity and false positive rate is that all epochs are treated in the same manner without taking into consideration the epoch length. In this way, one SWD epoch of 10 sec length will contribute the same as an epoch of 1 sec. Given this consideration, sensitivity and specificity can be defined based on the cumulative SWD time or “cumulative epileptiform burden.” In this case, sensitivity is defined as the cumulative detected time (in sec) over the total time, whereas the false positive rate is defined as the cumulative missed seizure time over the corresponding time of the recordings.

The ROC curves for the four rats and the mean curve for all four rats can be seen in Fig. 5(C&D). The fact that the ROC curve using the cumulative time (Fig. 5B) has higher sensitivity values compared to the that with the detected number of epochs (Fig. 5D) means that the missed epochs are shorter compared to the detected epochs. This is consistent with previous results in absence epilepsy detection [19]. It is worth mentioning that in the current study we considered SWD epochs of all lengths. In clinical practice, a frequently encountered issue is whether SWDs are sufficiently long to result in an absence seizure (e.g., a 0.5-sec SWD epoch would not be clinically significant). Under such assumptions, the detection sensitivity and false positive rate would improve drastically. Therefore, the error analysis presented here can be viewed as an upper limit of the error range. With regard to the second parameter of the algorithm (low threshold), it determines the accuracy of the seizure onset and offset detection. It is easy to recognize from Fig. 5 that changes of the low threshold would modify the onset and offset detection point by some number of sample points, which correspond to 1/200 sec each.

Fig. 5. (A) ROC for four individual rats using number of epochs (B) the average curve for all rats using number of epochs (C) ROC for four individual rats using length of epochs (D) the average curve for all rats using length of epochs.



IV. DISCUSSION AND CONCLUSIONS

In this paper, we presented an adaptation of the algorithm proposed for human absence epilepsy [19] for the detection of SWDs in rat model of absence epilepsy. The proposed algorithm is robust with respect to the input parameters, which means that the output (detected epochs) cannot differ significantly when small changes are made to the threshold parameters. In addition, the ROC analysis shows that high sensitivity rates ($\sim >90\%$) can be achieved along with a low false positive rate ($\sim 2-4$ false positive epochs per hour). When considering the cumulative time of the SWD epochs instead of the absolute number of the epochs, the algorithm demonstrates, on average, over 90% accuracy while the total missed SWD time doesn't exceed 8.5 sec per hour. Importantly, the sensitivity percentages and the false positive rates can increase dramatically when epochs longer than some predefined duration are considered. However, an optimal threshold parameter cannot be proposed because the desired sensitivity and false positive rate are highly application-dependent. These results encourage us to generalize the detection methodology into other generalized EEG patterns that appear in specific frequency bands while further investigation and experiments are ongoing to reveal potential imperfections of the algorithm.

ACKNOWLEDGMENT

We would like to acknowledge NSF and Air Force for partial financial support. This work was partially supported by the North Florida Foundation for Research and Education Inc., North Florida/South Georgia Veterans Health System, by an Epilepsy Foundation Research Initiative for Seniors Award (SPN), and NINDS R01 NS046015 (KMK). We would also like to acknowledge Pennsylvania Department of Health Research for the Formula Fund RFA 04-07-09 SAP 4100031268 (KMK).

REFERENCES

- [1] N. Ahuja, S. Lertrattanapanich, and N. K. Bose. Properties determining choice of mother wavelet. *Vision, Image and Signal Processing, IEE Proceedings*, 2005.
- [2] G. Buzsáki, A. Smith, S. Berger, L. J. Fisher, and F. H. Gage. Petit mal epilepsy and parkinsonian tremor: hypothesis of a common pacemaker. *Neuroscience* 36(1):1-14 1990.
- [3] A. M. Coenen, W. H. Drinkenburg, M. Inoue, and E. L. van Luijtelaar. Genetic models of absence epilepsy, with emphasis on the WAG/Rij strain of rats. *Epilepsy Research* 12(2):75-86 1992.
- [4] E. Faselow, A. P. Reid, and M.A.L. Nicoletis. Reduction of pentylentetrazole-induced seizure activity in awake rats by seizure-triggered trigeminal nerve stimulation. *The Journal of Neuroscience*, 20:8160-8, 2000.
- [5] K. M. Kelly. Spike-wave discharges: absence or not, a common finding in common laboratory rats. *Epilepsy Currents* 4(5): 176-177 2004.
- [6] K. M. Kelly, A. Kharlamov, T. M. Hentosz, E. A. Kharlamov, J. M. Williamson, E. H. Bertram, J. Kapur, and D.M. Armstrong. Photothrombotic brain infarction results in seizure activity in aging Fischer 344 and Sprague Dawley rats. *Epilepsy Research* 47: 189-203 2001.
- [7] K. M. Kelly, P. I. Jukkola, E. A. Kharlamov, K. L. Downey, J. W. McBride, R. Strong, and J. Aronowski. Long-term video-EEG recordings following transient unilateral middle cerebral and common carotid artery occlusion in Long-Evans rats. *Experimental Neurology* 201: 495-506 2006.
- [8] E. A. Kharlamov, P. I. Jukkola, K. L. Schmitt, and K. M. Kelly. Electrophysiological characteristics of epileptic rats following photothrombotic brain infarction. *Epilepsy Research* 56: 185-203 2003.
- [9] S. P. Nair, P. I. Jukkola, M. Quigley, A. Wilberger, D. S. Shiau, J. C. Sackellares, P. M. Pardalos, and K. M. Kelly. Absence seizures as resetting mechanisms of brain dynamics. *Cybernetics and Systems Analysis* 44(5):664-672 2008.
- [10] P.M. Pardalos, V. Boginski, and A. Vazacopoulos, editors. Data Mining in Biomedicine, volume 7 of Springer Optimization and Its Applications. Springer Verlag, 2007.
- [11] P.M. Pardalos, J.C. Sackellares, P.R. Carney, and L.D. Iasemidis, editors. Quantitative Neuroscience: Models, Algorithms, Diagnostics, and Therapeutic Applications. Springer Verlag, 2004
- [12] K. Semba, H. Szechtman, and B. R. Komisaruk. Synchrony among rhythmical facial tremor, neocortical 'alpha' waves, and thalamic non-sensory neuronal bursts in intact awake rats. *Brain Research* Aug 18;195(2):281-98 1980.
- [13] O. Seref, E.O. Kundakcioglu, and P.M. Pardalos, editors. Data Mining, Systems Analysis, and Optimization in Biomedicine, volume 953 of AIP Conference Proceedings. American Institute of Physics, 2007.
- [14] E. L. Van Luijtelaar, Coenen AM. Two types of electrocortical paroxysms in an inbred strain of rats. *Neuroscience Letters* Oct 20;70(3):393-7 1986.
- [15] P. Van Hese, J.P. Martens, P. Boon, S. Dedeurwaerdere, I. Lemahieu, and R. Van de Walle. Detection of spike and wave discharges in the cortical EEG of genetic absence epilepsy rats from Strasbourg. *Physics in Medicine and Biology*, 48:1685-700, 2003.
- [16] M. Vergnes, C. Marescaux, G. Micheletti, J. Reis, A. Depaulis, L. Rumbach, and J. M. Warter. Spontaneous paroxysmal electroclinical patterns in rat: a model of generalized non-convulsive epilepsy. *Neuroscience Letters* Nov 16;33(1):97-101 1982.
- [17] F. Westerhuis, W. Van Schaijk, and G. Van Luijtelaar. Automatic detection of spike-wave discharges in the cortical EEG of rats. *Measuring Behavior '96, Int. Workshop on Methods and Techniques in Behavioral Research*, Utrecht, The Netherlands 16-18 Oct. 1996.
- [18] J. O. Willoughby and L. Mackenzie. Nonconvulsive electrocorticographic paroxysms (absence epilepsy) in rat strains. *Lab Anim Sci*. Dec;42(6):551-4 1992.
- [19] P. Xanthopoulos, S. Rebennack, C. C. Liu, P.M. Pardalos, G. L. Holmes and B. M. Uthman. A novel wavelet based algorithm for spike and wave detection in absence epilepsy. Submitted 2008